Journal of Non-Crystalline Solids 357 (2011) 397–400

Contents lists available at ScienceDirect

Journal of Non-Crystalline Solids

journal homepage: www.elsevier.com/ locate/ jnoncrysol

Heterogeneous slow dynamics and the interaction potential of glass-forming liquids

D. Coslovich [a,*], C.M. Roland [b]

[a] Institut für Theoretische Physik, Technische Universität Wien, Vienna, Austria
[b] Naval Research Laboratory, Washington DC, USA

ARTICLE INFO

Article history:
Received 17 April 2010
Received in revised form 27 July 2010
Available online 26 August 2010

Keywords:
Density scaling;
Fragility;
Dynamic heterogeneity;
Pressure-energy correlations;
Lennard-Jones potential;
Mixtures;
Network glass

ABSTRACT

The role of the intermolecular interaction potential on the dynamic and thermodynamic properties of model glass-forming mixtures is investigated through molecular dynamics simulations. Variations of the repulsive exponent m in the well-studied Lennard-Jones Kob-Andersen mixture are shown to have a negligible effect on the fragility and dynamic correlation volumes when quenches are performed at constant pressure. The number of dynamically correlated particles, estimated from the temperature derivative of a two-point dynamic correlation function, is approximately invariant to m at any fixed relaxation time. Further, the density scaling property of a model tetrahedral network glass-former, based on inverse power law and Lennard-Jones potentials, is investigated. The optimal scaling exponent γ is close to zero and does not superpose the data well. The breakdown of density scaling is consistent with the absence of correlation between fluctuations of the virial and the potential energy. These results emphasize the crucial role of structural many-body correlations in glass-forming systems and show the need of investigations of more complex and realistic model liquids.

1. Introduction

The divergence in their properties as liquids approach vitrification is among the most fascinating phenomena of the physical world. A one degree change in temperature can alter structural relaxation times by decades, corresponding to activation energies two or more orders of magnitude larger than van der Waals bond energies. Although a predictive, first-principles theory of the glass transition remains elusive, much progress has been made in understanding the relaxation behavior. Recent progress has drawn on the pioneering work of Hoover and Ross [1], who showed that when the intermolecular potential is a repulsive inverse power law (IPL),

$$u(r) \sim r^{-m} \tag{1}$$

where r is the particle separation and m is a constant, excess thermodynamic properties are uniquely determined by the quantity ρ^γ/T, where ρ is density, T is temperature, and γ is a material constant. Subsequently, molecular dynamics (MD) simulations showed this scaling property to apply to diffusion constants of Lennard-Jones (LJ) particles [2]. In consideration of the "local" nature of reorientational motions in supercooled liquids, in which intermolecular distances are limited primarily to the repulsive range of r, the scaling was extended to real materials [3,4], and for non-associated, organic liquids and polymers the dynamics in the viscous regime indeed conform to a scaling relation, $\tau \sim f(\rho^\gamma/T)$ (see [5] and references therein). Recently, MD simulations affirmed the putative connection between this scaling property and the intermolecular potential; specifically, the value of γ superposing diffusion constants or relaxation times was found to be equal to the effective slope of the repulsive part of $u(r)$ in the vicinity of its minimum [6]. However, this slope is larger than m in Eq. (1) due to the influence of the attractive term (its decay with decreasing r causes the potential to be steeper than the bare repulsive term).

The scaling relation describes the effect of thermodynamic variables on macroscopic observables (diffusion constant, relaxation time, viscosity), but of course supercooled liquids are in dynamic equilibrium, characterized by thermal fluctuations about these mean values. Pedersen et al. [7] discovered that for many simulated liquids, such fluctuations in the potential energy and the virial are linearly correlated, with a proportionality constant numerically equal to the scaling exponent γ. For a strict IPL material, the correlation is exact; for real liquids or LJ particles, the correlation of U and W supports the IPL with an added linear term as a reasonable approximation to the interaction potential [8]. However, the existence of this correlation is not a sufficient condition to guarantee conformance to the scaling relation [9]. Gnan et al. [10] have coined the term "isomorph" to describe thermodynamic pathways along which properties of a liquid remain constant; an operative definition is pathways defined by constancy of ρ^γ/T, where γ can be estimated from equilibrium U–W fluctuations.

Thermal fluctuations are central to the supercooled behavior of liquids. In the ultra-viscous state the dynamics is inherently

* Corresponding author.
E-mail addresses: coslovich@cmt.tuwien.ac.at (D. Coslovich), roland@nrl.navy.mil (C.M. Roland).

0022-3093/$ – see front matter © 2010 Elsevier B.V. All rights reserved.
doi:10.1016/j.jnoncrysol.2010.07.050

heterogeneous, with many theories of the glass transition positing a growing length scale of dynamic correlations as the origin of vitrification. We recently showed both from MD simulations [9] and experimentally [11] that the number of particles (molecules) within a correlation volume, N_c, is determined by the relaxation time. Since the latter is a function of ρ^γ/T, this means that N_c follows the same scaling relation, $N_c = g(\rho^\gamma/T)$. The question arises: what aspects of the intermolecular potential are related to dynamic heterogeneity? This is an important issue, potentially revealing how molecular structure governs the dynamic correlations and hence the magnitude of τ.

One reflection of dynamic heterogeneity is the distribution of structural and reorientational relaxation times, whose mean value is τ. This distribution can be characterized by the stretching exponent, β_K, in the Kolhrausch function used to describe the shape of the relaxation function. Smaller β_K implies a broader distribution and ostensibly a more heterogeneous dynamics. Interestingly, at any given value of τ, β_K is fixed [12]; moreover, since β_K is linearly correlated with the fragility, i.e., $dlog(\tau)/d(T_g/T)$ evaluated at $T = T_g$ [13], it is tempting to posit a mutual correlation of N_c with both β_K and fragility. Since these quantities are all connected to the scaling relation [12–14], the possibility exists to interpret these properties in terms of the forces between molecules, given the connection of the scaling exponent γ to the intermolecular potential [6,15]. However, prior studies are inconclusive. De Michele et al. [16] found that for particles interacting according to an IPL, the fragility was unaffected by the value of m (Eq. (1)). On the other hand, Bordat et al. [17] included an attractive term in the pair potential and found that fragility increased with the anharmonicity of the potential energy. The uncertainty of these studies carries over to efforts to correlate the nonergodicity factor in the low temperature limit, and hence the curvature of the minimum in the potential for the glass, with a liquid's fragility [18,19].

In this work we study the dynamics of modified LJ mixtures with pair potentials [17]

$$u_{\alpha\beta}(r) = \frac{E_{\alpha\beta}}{m-6}\left[6\left(\frac{r_{\alpha\beta}}{r}\right)^m - m\left(\frac{r_{\alpha\beta}}{r}\right)^6\right] \tag{2}$$

where α and β are species indices, $r_{\alpha\beta}$ and $E_{\alpha\beta}$ are material-specific interaction parameters, and the repulsive exponent m was varied as $8 \le m \le 36$. From simulations at constant pressure (mimicking the common experimental protocol), we find that the steepness of $u_{\alpha\beta}(r)$ has practically no effect on either the isobaric fragility or the stretching exponent, and that N_c at any fixed τ is also independent of m. Previously, conformance to scaling and the properties that ensue therefrom has been found primarily for non-associated organic molecules. We include herein MD results for a tetrahedral network glass. Notwithstanding that the force-field is based on IPL and LJ potentials, this system exhibits a breakdown of ρ^γ/T scaling and accordingly an absence of correlation between the potential energy and the virial. These results agree with earlier work of Le Grand et al. [20] on simulated silica, and emphasize the intimate connection between structural correlations and dynamic scaling behavior.

2. Results

In the following we will initially focus on molecular dynamics simulations of a modified version of the well-known Kob-Andersen Lennard-Jones mixture [21] based on Eq. (2). The systems studied herein are composed of $N = N_1 + N_2 = 1000$ particles in a cubic cell with periodic boundary conditions. In our simulations the repulsive exponent m is varied for all pairs $\alpha-\beta$, maintaining the same ratios $r_{\alpha\beta}/r_{11}$ and $E_{\alpha\beta}/E_{11}$ as in the original model. A smooth cut-off scheme [22] is employed to ensure continuity up to the first derivative of the potential at the cut-off $r_c = 2.5\times 2^{1/6} r_{\alpha\beta}$. Standard reduced Lennard-Jones units are used throughout [23]. The pair potentials $u_{11}(r)$ for the different m are plotted in Fig. 1. Increasing m not only affects the steepness of the potential but also increases the "coupling" [17], i.e., the inverse width of $u_{\alpha\beta}(r)$. The effect of a similar variation of $u_{11}(r)$ has been studied in [17] for a modified Kob-Andersen mixture at constant density. However, the simulations reported herein were carried out at constant pressure, $P = 10$, by coupling the system to a Berendsen thermostat and a Berendsen barostat during equilibration. Production runs were performed using the Nose-Poincare thermostat [24]. Equilibration criteria were similar to the ones used in previous simulations of Lennard-Jones mixtures [25,26]. To improve the statistics and to average out small discrepancies in the actual pressure, three independent realizations were considered.

In Fig. 2 we show the density of the system as a function of temperature for varying m. The density shifts systematically to smaller values as m is increased at constant pressure. That is, as m increases at fixed temperature, smaller densities are enforced to achieve the same pressure value, due to the increased coupling of the potential. This suggests a different role of thermal activation and jammed dynamics when varying m.

Arrhenius plots of the isobaric relaxation times, defined from the decay to $1/e$ of the self-intermediate scattering function

$$F_s(k,t) = \frac{1}{N}\sum_{j=1}^{N} \langle exp\left\{i\mathbf{k}\cdot\left[\mathbf{r}_j(t) - \mathbf{r}_j(0)\right]\right\}\rangle \tag{3}$$

are shown in Fig. 3 (upper panel) for these systems. Following previous work [17], we evaluate $F_s(k,t)$ at a wave-vector $k^* = 2\pi/r^*$, where r^* is the position of the first peak in the radial distribution function $g_{11}(r)$. At any given temperature there is a systematic increase in τ with increasing steepness of the repulsive potential; however, when plotted versus the T_O-normalized temperature, where T_O is the characteristic temperature at which relaxation departs from single exponential decay [27], the data collapse to essentially a single curve (lower panel of Fig. 3). A close inspection of the T-dependence of the relaxation times suggests a slight increase of fragility by increasing m, although the present data do not allow drawing a firm conclusion. Thus, the isobaric fragility of the systems is essentially independent on the steepness of the potential, when comparisons are made at constant well depth. A comparison with the results of Bordat et al. [17] indicates, therefore, that the effect of the intermolecular potential on dynamical properties may depend on the conditions—isochoric or isobaric—under which a liquid is quenched. Finally, in accord with the well-established correlation of fragility with the stretching of the relaxation function, the exponent β_K obtained from stretched exponential fits to the self-intermediate scattering functions also superpose as a function of T_O/T (data not shown).

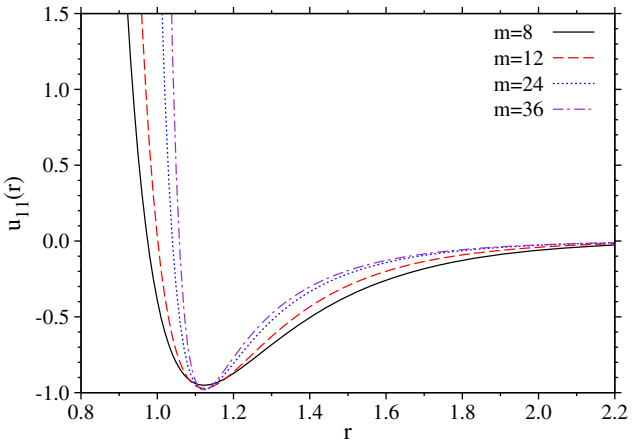

Fig. 1. Pair potential $u_{11}(r)$ (Eq. (2)) for different values of m. The small discrepancies between the values at the minimum are due to the smooth cut-off employed.

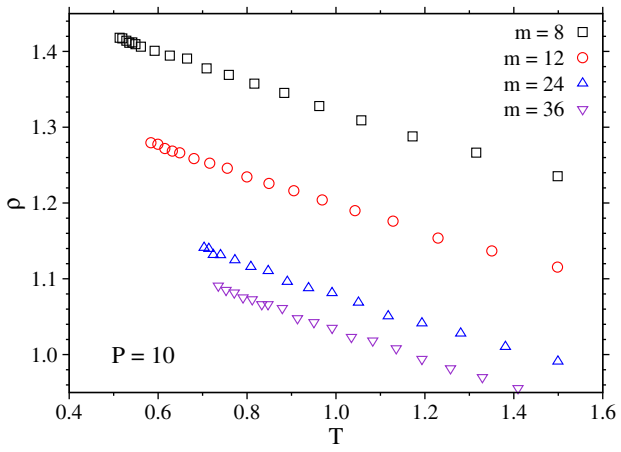

Fig. 2. Density ρ as a function of temperature T for different values of m at constant pressure $P=10$.

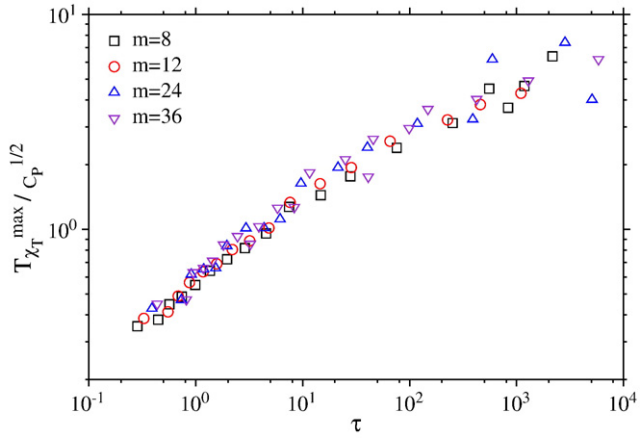

Fig. 4. Lower bound to N_{corr} (Eq. (5)) as a function of relaxation times τ for different values of m. The wave-vector at which χ_T is evaluated is the same as in Fig. 3.

The spatial extent of the correlation of the motions in viscous liquids over a time-span t is described by the four-point dynamic susceptibility

$$\chi_4(t) = N\left[<f_s^2(k,t)> - F_s^2(k,t)\right] \tag{4}$$

having a maximum value, χ_4^{max}, equal to N_c. In Eq. (4) $f_s(k,t)$ is the instantaneous value of the self-intermediate scattering function, whose time average is $<f_s(k,t)>=F_s(k,t)$. Previously we calculated χ_4 for LJ particles with $m=12$ [9]. As shown by Berthier and coworkers [28], however, the four-point dynamic susceptibility can be approximated by the temperature derivative of a two-point dynamic correlation function

$$\chi_4(t) \geq \frac{T^2}{c_P}\chi_T^2(t) = \frac{T^2}{c_P}\left(\frac{\partial \Phi(t)}{\partial T}\right)^2 \tag{5}$$

where $\Phi(t)$ is a two-point, time-dependent correlation function and c_P the isobaric heat capacity. In the following, we use $\Phi(t)=F_s(k^*,t)$ and consider the variation of the maximum of χ_T as a function of temperature, as in recent studies [11,28–30].

In prior work we found that N_c for a given material (defined in simulations by a particular value of m) depends only on the magnitude of τ, independent of T or ρ [9]. Moreover, experimental N_c for *different* materials collapse onto a single curve at shorter values of the relaxation times ($\tau<10^{-8}$s) [11]; however, with decreasing T (or increasing ρ) these N_c show substantial differences for different materials compared at fixed τ. In Fig. 4 we plot the χ_T approximation of N_c (Eq. (5)) for particles of species 1 in the Kob-Andersen mixture with varying m. There is only a small increase of roughly 30% in N_c at fixed τ as m increases from 8 to 36. This change is on the order of the scatter in the calculations and thus barely significant. Preliminary

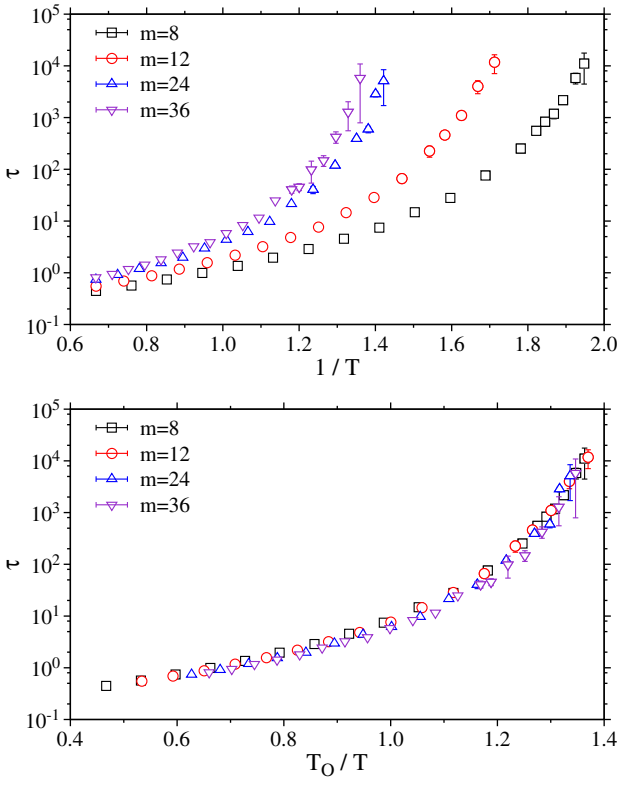

Fig. 3. Arrhenius plots of relaxation times τ from the self-intermediate scattering function $F_s(k=k^*,t)$. The wave-vector k^* is chosen such that $k^*=2\pi/r^*$, where r^* is the position of the first peak in the radial distribution function $g_{11}(r)$: the corresponding values of k^* are 6.2 ($m=8$), 6.0 ($m=12$), 5.8 ($m=24$), and 5.7 ($m=36$). Results are shown for isobaric quenches at $P=10$. Upper panel: τ versus $1/T$. Lower panel: τ versus T_O/T, where T_O is the onset temperature of non-exponential relaxation of $F_s(k^*,t)$. The values of T_O are 0.70 ($m=8$), 0.80 ($m=12$), 0.94 ($m=24$), and 0.99 ($m=36$).

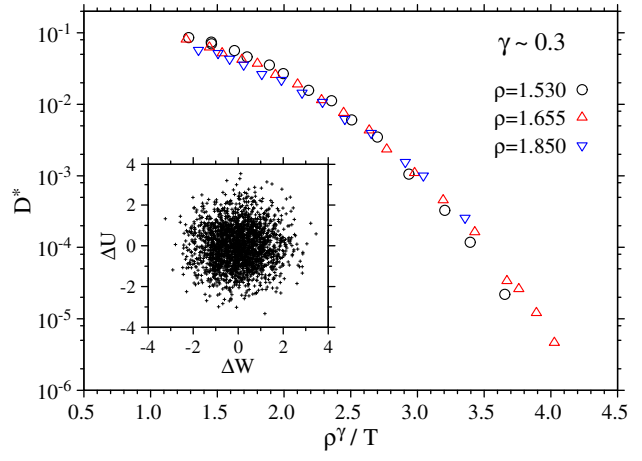

Fig. 5. Main plot: reduced diffusion coefficients $D^*=\rho^{-1/3}T^{-1/2}D$ of the network glass [31] as a function of ρ^γ/T for different densities and $\gamma\sim0.3$. Inset: normalized fluctuations of the potential energy ΔU versus normalized fluctuations of the virial ΔW for the state point $\rho=1.655$, $T=0.29$.

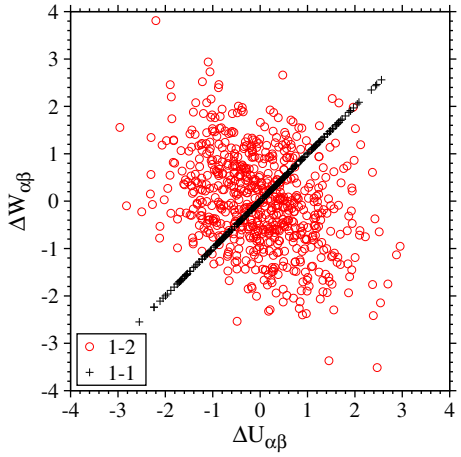

Fig. 6. Correlation between partial contributions to virial fluctuations, $\Delta W_{\alpha\beta}$, and potential energy fluctuations, $\Delta U_{\alpha\beta}$, obtained by summing only terms of W and U originating from $\alpha-\beta$ pairs of particles. Results are shown for the network glass model at $\rho=1.655$ and $T=0.29$ for 1–1 (crosses) and 1–2 (circles) pairs.

results for an additive, symmetric mixture confirm the insensitivity of N_c to m at constant pressure.

Finally, we consider a simple model of a network glass-former [31], in which particles interact through the potential

$$u_{\alpha\alpha}(r) = 4\epsilon_{\alpha\alpha}\left(\frac{\sigma_{\alpha\alpha}}{r}\right)^{12} \tag{6}$$

$$u_{\alpha\beta}(r) = 4\epsilon_{\alpha\beta}\left[\left(\frac{\sigma_{\alpha\beta}}{r}\right)^{12}-\left(\frac{\sigma_{\alpha\beta}}{r}\right)^{6}\right], \quad \alpha\neq\beta \tag{7}$$

where α, $\beta=1$, 2 are indexes of species. The optimal non-additive parameters that reproduce a tetrahedral network structure for a reduced density $\rho\approx1.65$ (close to the experimental density of silica) and the details of the simulations can be found in [31]. The force-field is based on IPL and LJ potentials and thus it might be expected that this network glass will inherit general properties associated with IPL-like potentials, e.g. density scaling and U–W correlations. In Fig. 5 the diffusion coefficient of particles of species 1 during isochoric quenches are plotted as a function of ρ^{γ}/T. The optimal value of this scaling variable, $\gamma\sim0$, is unphysical in view of a generalized IPL approximation [8] and moreover there are systematic (albeit small) deviations from superpositioning of the data. The breakdown of the ρ^{γ}/T scaling is accompanied by a striking lack of correlation between the (normalized) fluctuations of W and U. This is exemplified in the inset of Fig. 5 for a selected state point at low temperature, at which the liquid displays a nearly ideal tetrahedral network structure ($\rho=1.655$, $T=0.29$). More generally, the estimated Pearson correlation coefficient R remains below 0.1 over the whole investigated range of state parameters.

The absence of U–W correlations is elucidated in Fig. 6, where we show, for the same selected state point considered above, the partial, species-dependent contributions $\Delta W_{\alpha\beta}$ and $\Delta U_{\alpha\beta}$ to virial and potential energy fluctuations, respectively. Contributions arising from $u_{11}(r)$ (and $u_{22}(r)$, not shown) show perfect correlation, as expected for IPL potentials. In contrast, no correlation is found for the 1–2 pairs, whose interaction is described by a simple LJ potential. Thus our results emphasize how U–W correlations are indeed a necessary condition in order for density scaling to apply and that such correlations may arise, in general, from non-trivial many-body effects.

3. Conclusion

Previously it was known both from simulations and experiments that the fragility, Kohlrausch exponent, and the number of dynamic correlating molecules are constant at a fixed value of the relaxation time for a given material. Herein we determined that for different model glass-forming systems, defined by the exponent of the repulsive term in their respective pair potentials, this constancy of the fragility, β_K, and N_c at fixed τ under isobaric conditions is maintained to a good approximation. Moreover, these quantities are invariant to the value of the repulsive exponent; thus, the variations in these properties seen among different real materials have their origin in other aspects of the intermolecular potentials, with the many-body character of interparticle distances and forces having a role in the heterogeneous dynamics.

Acknowledgement

D. C. acknowledges financial support by the Austrian Science Fund (FWF) (Project number: P19890-N16). The work at NRL was supported by the Office of Naval Research.

References

[1] W.G. Hoover, M. Ross, Contemp. Phys. 12 (1971) 339.
[2] Y. Hiwatari, H. Matsuda, T. Ogawa, N. Ogita, A. Ueda, Prog. Theor. Phys. 52 (1974) 1105.
[3] A. Tölle, Rep. Prog. Phys. 65 (2001) 1473.
[4] A.G.S. Hollander, K.O. Prins, J. Non-Cryst. Solids 286 (2001) 1.
[5] C.M. Roland, S. Hensel-Bielowka, M. Paluch, R. Casalini, Rep. Prog. Phys. 68 (2005) 1405.
[6] D. Coslovich, C.M. Roland, J. Phys. Chem. B 112 (2008) 1329.
[7] U.R. Pedersen, N.P. Bailey, T.B. Schrøder, J.C. Dyre, Phys. Rev. Lett. 100 (2008) 015701.
[8] N.P. Bailey, U.R. Pedersen, N. Gnan, T.B. Schrøder, J.C. Dyre, J. Chem. Phys. 129 (2008) 184508.
[9] D. Coslovich, C.M. Roland, J. Chem. Phys. 131 (2009) 151103.
[10] N. Gnan, T.B. Schrøder, U.R. Pedersen, N.P. Bailey, J.C. Dyre, J. Chem. Phys. 131 (2009) 234504.
[11] D. Fragiadakis, R. Casalini, C.M. Roland, J. Phys. Chem. B 113 (2009) 13134.
[12] K.L. Ngai, R. Casalini, S. Capaccioli, M. Paluch, C.M. Roland, J. Phys. Chem. B 109 (2005) 17356.
[13] R. Bohmer, K.L. Ngai, C.A. Angell, D.J. Plazek, J. Chem. Phys. 99 (1993) 4201.
[14] R. Casalini, C.M. Roland, Phys. Rev. B 71 (2005) 014210.
[15] C.M. Roland, S. Bair, R. Casalini, J. Chem. Phys. 125 (2006) 124508.
[16] C. De Michele, F. Sciortino, A. Coniglio, J. Phys. Condens. Matter 16 (2004) L489–L494.
[17] P. Bordat, F. Affouard, M. Descamps, K.L. Ngai, Phys. Rev. Lett. 93 (2004) 105502.
[18] T. Scopigno, G. Ruocco, F. Sette, G. Monaco, Science 302 (2003) 849.
[19] K. Niss, C. Dalle-Ferrier, V.M. Giordano, G. Monaco, B. Frick, C. Alba-Simionesco, J. Chem. Phys. 129 (2008) 194513.
[20] A.L. Grand, C. Dreyfus, C. Bousquet, R.M. Pick, Phys. Rev. E 75 (2007) 061203.
[21] W. Kob, H.C. Andersen, Phys. Rev. E 52 (1995) 4134.
[22] S.D. Stoddard, J. Ford, Phys. Rev. A 8 (1973) 1504.
[23] M.P. Allen, D.J. Tildesley, Computer Simulation of Liquids, Clarendon Press, Oxford, 1987.
[24] S. Nosé, J. Phys. Soc. Jpn. 70 (2001) 75.
[25] D. Coslovich, G. Pastore, J. Chem. Phys. 127 (2007) 124505.
[26] D. Coslovich, G. Pastore, J. Chem. Phys. 127 (2007) 124504.
[27] S. Sastry, P.G. Debenedetti, F.H. Stillinger, Nature 393 (1998) 554.
[28] L. Berthier, G. Biroli, J.-P. Bouchaud, L. Cipelletti, D.E. Masri, D. L'Hôte, F. Ladieu, M. Pierno, Science 310 (2005) 1797.
[29] C. Dalle-Ferrier, C. Thibierge, C. Alba-Simionesco, L. Berthier, G. Biroli, J.-P. Bouchaud, F. Ladieu, D. L'Hôte, G. Tarjus, Phys. Rev. E 76 (2007) 041510.
[30] S. Capaccioli, G. Ruocco, F. Zamponi, J. Phys. Chem. B 112 (2008) 10652.
[31] D. Coslovich, G. Pastore, J. Phys. Condens. Matter 21 (2009) 285107.